



TITLE:

Characterization of a thermostable 2,4-diaminopentanoate dehydrogenase from *Fervidobacterium nodosum* Rt17-B1.

AUTHOR(S):

Fukuyama, Sadanobu; Mihara, Hisaaki; Miyake, Ryoma; Ueda, Makoto; Esaki, Nobuyoshi; Kurihara, Tatsuo

CITATION:

Fukuyama, Sadanobu ...[et al]. Characterization of a thermostable 2,4-diaminopentanoate dehydrogenase from *Fervidobacterium nodosum* Rt17-B1.. *Journal of bioscience and bioengineering* 2014, 117(5): 551-556

ISSUE DATE:

2014-05

URL:

<http://hdl.handle.net/2433/187042>

RIGHT:

© 2013 The Society for Biotechnology, Japan. Published by Elsevier B.V.; この論文は出版社版ではありません。引用の際には出版社版をご確認ご利用ください。 ; This is not the published version. Please cite only the published version.

1 Characterization of a thermostable 2,4-diaminopentanoate dehydrogenase from *Fervidobacterium*
2 *nodosum* Rt17-B1

3
4 Sadanobu Fukuyama,¹ Hisaaki Mihara,¹ Ryoma Miyake,^{2,3} Makoto Ueda,^{2,3} Nobuyoshi Esaki,¹ and
5 Tatsuo Kurihara^{1,*}

6 ¹Institute for Chemical Research, Kyoto University, Uji, Kyoto 611-0011, Japan

7 ²Mitsubishi Chemical Group Science and Technology Research Center, Inc., Yokohama 227-8502,
8 Japan

9 ³API Corporation, Yokohama 227-8502, Japan

10
11 *Corresponding author. Tel: +81-774-38-4710, Fax: +81-774-38-3248, E-mail:
12 kurihara@scl.kyoto-u.ac.jp

13
14 Present addresses.

15 S. F.: KOGA ISOTOPE, Ltd., Koka, Shiga 520-3404, Japan

16 H. M.: Department of Biotechnology, College of Life Sciences, Ritsumeikan University, Kusatsu,
17 Shiga 525-8577, Japan

18 M. U.: Department of Materials Chemistry and Bioengineering, Oyama National College of
19 Technology, Oyama, Tochigi 323-0806, Japan

20
21 Running title: Thermophilic 2,4-diaminopentanoate dehydrogenase

22
23 Key words: 2,4-diaminopentanoate dehydrogenase; *Fervidobacterium nodosum*; amino acid
24 dehydrogenase; ornithine metabolism; deamination; amination; thermophilic enzyme

27 Abstract

28 2,4-Diaminopentanoate dehydrogenase (2,4-DAPDH), which is involved in the oxidative
29 ornithine degradation pathway, catalyzes the NAD^+ - or NADP^+ -dependent oxidative deamination of
30 (2*R*, 4*S*)-2,4-diaminopentanoate (2,4-DAP) to form 2-amino-4-oxopentanoate. A *Fervidobacterium*
31 *nodosum* Rt17-B1 gene, *Fnod_1646*, which codes for a protein with sequence similarity to
32 2,4-DAPDH discovered in metagenomic DNA, was cloned and overexpressed in *Escherichia coli*, and
33 the gene product was purified and characterized. The purified protein catalyzed the reduction of NAD^+
34 and NADP^+ in the presence of 2,4-DAP, indicating that the protein is a 2,4-DAPDH. The optimal pH
35 and temperature were 9.5 and 85°C, respectively, and the half-denaturation time at 90°C was 38 min.
36 Therefore, the 2,4-DAPDH from *F. nodosum* Rt17-B1 is an NAD(P)^+ -dependent thermophilic-alkaline
37 amino acid dehydrogenase. This is the first thermophilic 2,4-DAPDH reported, and it is expected to be
38 useful for structural and functional analyses of 2,4-DAPDH and for the enzymatic production of chiral
39 amine compounds. Activity of 2,4-DAPDH from *F. nodosum* Rt17-B1 was suppressed by 2,4-DAP via
40 uncompetitive substrate inhibition. In contrast, the enzyme showed typical Michaelis-Menten kinetics
41 toward 2,5-diaminohexanoate. The enzyme was uncompetitively inhibited by D-ornithine with an
42 apparent K_i value of 0.1 mM. These results suggest a regulatory role for this enzyme in the oxidative
43 ornithine degradation pathway.

44

45

46 Introduction

47 2,4-Diaminopentanoate dehydrogenase (2,4-DAPDH, EC 1.4.1.12) catalyzes NAD^{+} - or
48 NADP^{+} -dependent oxidative deamination of (2*R*, 4*S*)-2,4-diaminopentanoate (2,4-DAP) at carbon 4 to
49 form 2-amino-4-oxopentanoate (AKP) (1). In the 1970s, this enzyme was first discovered in a crude
50 extract of *Clostridium sticklandii* as a part of the oxidative ornithine degradation pathway (Fig. 1) (2-4),
51 and the genes implicated in this pathway were recently identified through a metagenomics approach in
52 an anaerobic digester from a wastewater treatment plant (5). The oxidative ornithine degradation
53 pathway has also been verified in several anaerobic genera, including *Clostridium*,
54 *Thermoanaerobacter*, *Propionibacterium*, and *Fervidobacterium*. The first step in this pathway is the
55 conversion of L-ornithine to the D isomer by ornithine racemase (6). D-Ornithine is then converted to
56 2,4-DAP by D-ornithine aminomutase (OAM), an adenosylcobalamine (AdoCbl) and pyridoxal
57 phosphate (PLP)-dependent enzyme, in which the amino group at carbon 5 is migrated to carbon 4 (7).
58 2,4-DAP is then oxidatively deaminated to form AKP. In the final step in this pathway, AKP undergoes
59 a thiolytic cleavage, which is catalyzed by AKP thiolase with coenzyme A, to form acetyl-CoA and
60 D-alanine (8).

61 Chiral amines are important starting materials for the synthesis of pharmaceuticals and
62 agrochemicals. To obtain these chiral amine compounds, a variety of chemical and enzymatic methods
63 have been utilized. Some examples include the enzymatic synthesis of chiral amines with lipases (9,
64 10) and ω -amino acid aminotransferases (11, 12). One drawback of most of these strategies is that they
65 require auxiliary compounds and involve multistep transformations. In addition, in synthesis methods
66 using an aminotransferase, the yield of the product is often unsatisfactory due to the reaction
67 equilibrium. These drawbacks may be overcome by using amino acid dehydrogenases. Amino acid
68 dehydrogenases catalyze the reduction of α -keto acids with concomitant amination of the substrates
69 with NAD(P)H and an ammonium ion. Therefore, these enzymes are useful for producing chiral
70 amines from the corresponding α -keto acid compounds in one step along with an established

71 NAD(P)H recycling system. The product yield might also be enhanced by increasing the concentration
72 of NAD(P)H with an NAD(P)H regeneration system. However, despite these advantages, the
73 applications for amino acid dehydrogenases have been limited to the production of α -amino acids.
74 2,4-DAPDH may expand the application range of amino acid dehydrogenases for the production of
75 other chiral amine compounds, because 2,4-DAPDH should catalyze the amination of the carbonyl
76 group at the γ position.

77 Thermostable enzymes from thermophilic organisms have been used extensively in industry
78 because these enzymes are inherently stable in harsh industrial processes. *Fervidobacterium* belongs
79 to the eubacterial order of *Thermotogales*, which includes the most extremely thermophilic eubacteria
80 presently known. It can grow at temperatures above 60°C with an optimal temperature of
81 approximately 80°C (13). In this study, we carried out gene cloning, overexpression, purification, and
82 biochemical characterization of a thermostable 2,4-DAPDH from the thermophilic anaerobic
83 bacterium, *Fervidobacterium nodosum* Rt17-B1. This is the first report of a thermophilic 2,4-DAPDH.
84 The role of this enzyme in the oxidative ornithine degradation pathway is also discussed.

85

86

87 Materials and Methods

88 *Materials*

89 Restriction enzymes and kits for genetic manipulation were obtained from Takara Bio
90 (Kyoto, Japan), New England Biolabs (Ipswich, MA), and Stratagene (La Jolla, CA). The pET14b
91 expression vector was purchased from Novagen (Madison, WI). His-bind Resin was obtained from
92 Novagen. All other reagents were of analytical grade and were from Nacalai Tesque (Kyoto, Japan)
93 and Wako Pure Chemical Industries (Osaka, Japan).

95 *Cloning of the 2,4-DAPDH gene from F. nodosum Rt17-B1*

96 Genomic DNA was isolated from *F. nodosum* Rt17-B1 (DSMZ, Braunschweig, Germany)
97 using a DNeasy Blood & Tissue Kit (Qiagen, Venlo, Netherlands) according to the manufacturer's
98 instructions. The gene encoding 2,4-DAPDH was amplified by overlap extension PCR to remove the
99 intrinsic NdeI site in the coding region. Two separate amplification reactions were performed using
100 Phusion DNA polymerase (Finnzymes, Espoo, Finland), 100 ng of genomic DNA as a template, and
101 the following two sets of primers: Fnod_1646 NdeI N
102 (5'-GCGGGAATTCCCATATGCGTATAGTTACTTGGGG-3') and Fnod_1646 deNdeI R
103 (5'-CATTTATCGCCAACCGTATGCTTTTGCTG-3') to amplify the DNA coding for the N-terminal
104 part of the protein, and Fnod_1646 deNdeI F (5'-CAGCAAAAGCATACGTTGGCGATAAATG-3')
105 and Fnod_1646 BamHI C (5'-GCCGCGGATCCTCATTCATTGAGAAAGGATTG-3') to amplify
106 the DNA coding for the C-terminal part of the protein. The underlined sequences indicate the
107 restriction sites for NdeI and BamHI, respectively. The double-underlined sequences indicate the sites
108 that anneal to the intrinsic NdeI site in the coding region. The PCR products were mixed and used as
109 templates in a second PCR to amplify the full-length gene using Fnod_1646 NdeI N and Fnod_1646
110 BamHI C. The amplified product was digested with NdeI and BamHI and inserted into the
111 corresponding sites of pET14b to generate an N-terminal His6-tagged protein. The recombinant

plasmid was designated pET_Fnod_DAPDH.

Expression and purification of 2,4-DAPDH

pET_Fnod_DAPDH was introduced into *Escherichia coli* Rosetta (DE3), and the cells were grown in LB medium containing 0.1 mM IPTG at 28°C for 15–17 h. The cells were harvested by centrifugation, resuspended in 50 mM Tris-HCl (pH 8.0), and homogenized by sonication. The homogenate was centrifuged at $25,000 \times g$ for 40 min at 4°C. The supernatant was loaded onto a His-bind column (10 mL) equilibrated with 50 mM Tris-HCl (pH 8.0). The enzyme was eluted with a 600-mL linear gradient of 0–500 mM imidazole in the same buffer. The enzyme fractions were pooled and dialyzed against 50 mM Tris-HCl (pH 8.0). The final preparation of the enzyme was stored at -80°C until use.

Synthesis of 2,4-DAP

2,4-DAP was obtained from D-ornithine by enzymatic synthesis using OAM. To prepare OAM, which is comprised of two subunits, OraS and OraE, the genes coding for these subunits were amplified by PCR from *F. nodosum* genomic DNA using the following two sets of primers:

FnodOAMS_N_Bam (5'-GGAGGGGATCCGATGAAACCAAGGCCG-3') and
FnodOAMS_C_Hind (5'-TTTCTTGGGTCGAGTTAAGCTTTTATTAC-3') for *oraS* and
FnodOAME_N_Nde (5'-GCGGTGAGTAACATATGGACAAAC-3') and FnodOAME_C_Xho
(5'-GAATTTGACTCGAGTTATTTTGTGAGATTC-3') for *oraE*. The underlined sequences indicate the restriction sites for BamHI, HindIII, NdeI, and XhoI, respectively. The *oraS* PCR product was digested with BamHI and HindIII and inserted into the corresponding sites of Multiple cloning site-1 of pCOLA Duet-1, and the *oraE* PCR product was digested with NdeI and XhoI and inserted into the corresponding sites of Multiple cloning site-2 of the same plasmid. The recombinant plasmid was designated pCOLA_Fnod_OAM.

137 *E. coli* Rosetta (DE3) cells harboring the expression plasmid pCOLA_Fnod_OAM were
138 grown in LB medium containing 0.1 mM IPTG at 28°C for 15–17 h. The cells were harvested by
139 centrifugation, resuspended in a 25-mM ACES buffer (pH 6.5), and homogenized by sonication. The
140 homogenate containing OAM was used to synthesize 2,4-DAP from D-ornithine.

141 The reaction mixture for the synthesis of 2,4-DAP consisted of 25 mM ACES buffer (pH
142 6.5), 50 mM D-ornithine, 50 μM PLP, 50 μM AdoCbl, 1 mM DTT, and the homogenate. The reaction
143 was performed in the dark on a magnetic stirrer plate at 55°C for 21 h. The reaction was terminated by
144 the addition of trichloroacetic acid (final concentration, 25%). After centrifugation and three ether
145 extractions, the extract was evaporated and taken up in water. The solution was desalted with a
146 Dowex-50W-X8, 200 to 400 mesh, H⁺-form column. After washing, the D-ornithine and 2,4-DAP
147 adsorbed to the column were eluted with 1 M NH₄OH. The D-ornithine and 2,4-DAP fractions were
148 pooled, evaporated, and reconstituted in chloroform:methanol:15% NH₄OH (36:46:20). D-Ornithine
149 and 2,4-DAP were then separated by column chromatography by using silicic acid (Silica Gel 60, 100
150 to 210 mesh; KANTO CHEMICAL, Tokyo, Japan) with chloroform:methanol:15% NH₄OH (36: 46:
151 20). The 2,4-DAP fractions were pooled and evaporated.

152

153 *Synthesis of 2,5-diaminohexanoate (2,5-DAH)*

154 2,5-DAH was obtained from D-lysine by enzymatic synthesis with lysine 5,6-aminomutase.
155 To obtain the enzyme, which is comprised of two subunits, KamD and KamE, the genes coding for
156 these subunits were amplified from *Thermoanaerobacter tengcongensis* genomic DNA by PCR using
157 the following two sets of primers: TTELAMa_N_Bam
158 (5'-GAGGGGATCCGATGAAGAAGAGCAAG-3') and TTELAMa_C_Sal
159 (5'-GGCGTCGACTCATCCTCTATCACCTCTT-3') for *kamD* and TTELAMb_N_Nde
160 (5'-GGTGATAGCATATGAACAGCGG-3') and TTELAMb_C_Xho
161 (5'-AATCGGCTCGAGTTATTTTTTATACCCTT-3') for *kamE*. The underlined sequences indicate

the restriction sites for BamHI, SalI, NdeI, and XhoI, respectively. The *kamD* PCR product was digested with BamHI and SalI and inserted into the corresponding sites in Multiple cloning site-1 of pCOLA Duet-1. The *kamE* PCR product was digested with NdeI and XhoI and inserted into the corresponding sites in Multiple cloning site-2 of the same plasmid. The recombinant plasmid was designated pCOLA_TTE_LAM.

E. coli Rosetta (DE3) cells harboring the expression plasmid pCOLA_TTE_LAM were grown in LB medium containing 0.1 mM IPTG at 28°C for 15–17 h. The cells were harvested by centrifugation, suspended in 25 mM PIPES buffer (pH 6.5), and homogenized by sonication. The homogenate containing lysine 5,6-aminomutase was used to synthesize 2,5-DAH from D-lysine.

The reaction mixture for the synthesis of 2,5-DAH consisted of 25 mM PIPES buffer (pH6.5), 50 mM D-lysine, 50 μM PLP, 50 μM AdoCbl, 1 mM DTT, and the homogenate. The reaction was performed in the dark on a magnetic stirrer plate at 55°C for 21 h. The reaction was terminated by the addition of trichloroacetic acid (final concentration, 25%). After centrifugation and three ether extractions, the supernatant was concentrated by evaporation and taken up in water. The solution was desalted by using a Dowex-50W-X8, 200 to 400 mesh, H⁺-form column. After washing, the D-lysine and 2,5-DAH adsorbed to the column were eluted with 1 M NH₄OH. The D-lysine and 2,5-DAH fractions were pooled, evaporated, and reconstituted in chloroform:methanol:15% NH₄OH (6:70:20). D-Lysine and 2,5-DAH were then separated by column chromatography using silicic acid (Silica Gel 60, 100 to 210 mesh; KANTO CHEMICAL) with chloroform:methanol:15% NH₄OH (6:70:20). The 2,5-DAH fractions were pooled and evaporated.

Enzyme assay

The activity of 2,4-DAPDH was determined spectrophotometrically by monitoring the change in A₃₄₀ upon the reduction of NAD⁺ at 55°C. The assay mixture consisted of 0.5 mM NAD⁺, 0.5 mM substrate, and 50 mM HEPES-NaOH (pH 8.5). The reaction was started by the addition of the

enzyme.

Determination of optimal pH and temperature

The pH optimum of the enzyme was determined using the following four buffer systems: 50 mM acetate buffer (pH 5–5.5), 50 mM potassium phosphate buffer (KPB) (pH 5.5–7), HEPES-NaOH buffer (pH 7–8.5), and CHES-NaOH buffer (pH 8.5–10). The optimal temperature of the enzyme was determined by measuring the enzyme activity over the temperature range of 5°C–95°C.

Determination of thermostability

The stability of the 2,4-DAPDH enzyme at elevated temperatures was investigated by incubating the enzyme in 50 mM HEPES-NaOH (pH 8.5) at 90°C and 100°C. At certain time intervals, samples were withdrawn, and the residual activity was measured under standard assay conditions.

Effect of metal ions and reagents

The effects of metal ions and various reagents on the enzyme were determined by measuring activity after incubating it in 50 mM HEPES-NaOH (pH 8.5) with and without different metal ions and reagents at 0.5 mM.

Determination of kinetic parameters

The initial rates of the enzyme reaction were measured while varying the concentration of one substrate while the concentration of the other substrate was held constant (and in excess). Data were fitted to the Michaelis-Menten equation, and the kinetic parameters were calculated using nonlinear least-squares regression with Kaleida Graph software (Adelbeck Software, Reading, PA). Substrate inhibition studies were performed with various concentrations of 2,4-DAP and a fixed saturating concentration of NAD⁺ (0.5 mM). The data were fitted to Equation 1, which is the standard

212 equation for complete uncompetitive substrate inhibition.

213
$$v = V_{\max} / \{1 + (K/[S]) + ([S]/K_i)\} \quad (\text{Equation 1})$$

214 In Equation 1, v and V_{\max} are the initial and maximum velocities, respectively, $[S]$ is the substrate
215 concentration, K is Michaelis constant for the substrate, and K_i is the inhibition constant for the
216 substrate.

217 Inhibitor studies of 2,4-DAPDH employed the assay described above. The kinetic analysis
218 was conducted with various concentrations of 2,4-DAP (0.01, 0.025, 0.05, 0.1, and 0.2 mM) and
219 D-ornithine (0.5, 1.5, and 2.0 mM). The K_i value was calculated from the Dixon plot.

220

221

Results

Identification and characterization of 2,4-DAPDH from F. nodosum Rt17-B1

To obtain a 2,4-DAPDH with superior thermostability, we focused on the thermophilic bacterium *F. nodosum* Rt17-B1. This strain was believed to have a functional oxidative degradation pathway for ornithine because it has *oraS* and *oraE* homologues that encode the S and E subunits of ornithine aminomutase, respectively. In the genome sequence of *F. nodosum*, the candidate gene for 2,4-DAPDH, *Fnod_1646* (GenBank accession number: ABS61481.1), is adjacent to the *oraS* and *oraE* homologues. The putative protein encoded by *Fnod_1646* is a homologue of the 2,4-DAPDH found in a metagenome from an anaerobic digester at a waste water-treatment plant (58.0% identity), which has been described as a homodimer with a subunit molecular mass of approximately 36 kDa that catalyzes the NAD⁺-dependent oxidation of 2,4-DAP to AKP. The protein encoded by *Fnod_1646* has a predicted molecular mass of 38 kDa and the GXGXXG sequence motif characteristic of the Rossmann fold, which is a typical of NAD(P)⁺-binding proteins.

To examine the enzyme activity of this protein, the *Fnod_1646* gene was cloned into the pET14b expression plasmid to construct pET_Fnod_DAPDH, and then heterologously expressed under the control of the T7 promoter in *E. coli* Rosetta (DE3) as an N-terminal His-tagged fusion. The gene product was purified in a single step by Ni-affinity chromatography. The homogeneity of the purified protein was verified by SDS-PAGE, which showed a single band with an apparent molecular mass of 38 kDa. In a reaction mixture containing 2,4-DAP, the purified protein catalyzed the reduction of NAD⁺ to NADH, indicating that the protein is a 2,4-DAPDH.

Optimal pH and thermostability

To determine the optimal pH for 2,4-DAPDH, the activity of the enzyme was measured at 55°C using 2,4-DAP as a substrate at pH 5.0–10. It showed maximum activity at pH 9.5 and high activity (>70% of maximum activity) at alkaline pHs in the range of 9.0–10.0 (Fig. 2). Enzymatic

activity was routinely determined at pH 8.5 (HEPES-NaOH buffer) in this study because NAD^+ is unstable at pH 9.0–10.0.

To determine the effect of temperature on enzyme activity, reactions were conducted using 2,4-DAP as a substrate in 50 mM HEPES-NaOH buffer (pH 8.5) over a temperature range of 5°C–95°C. The enzyme showed maximum activity at 85°C (Fig. 3). To test the thermostability of 2,4-DAPDH, the enzyme was incubated at 90°C and 100°C, and the residual activity was assayed. The half-life of the enzyme was estimated to be 38 min at 90°C and 2 min at 100°C (data not shown).

Effect of various reagents on 2,4-DAPDH activity

2,4-DAPDH activity was measured in the presence of EDTA and various divalent metal ions at a concentration of 0.5 mM (Table 1). EDTA did not affect 2,4-DAPDH activity. Mn^{2+} had no significant effect on 2,4-DAPDH activity, whereas Mg^{2+} , Ca^{2+} , Fe^{2+} , and Co^{2+} moderately inhibited the activity, and Ni^{2+} , Cu^{2+} , and Zn^{2+} almost completely inhibited the activity. Adding EDTA to the reaction mixture at a concentration equal to that of the metal ion completely suppressed the inhibition, indicating that these metals reversibly inactivated the enzyme (data not shown). K^+ and anions of the salts shown in Table 1 did not affect enzyme activity.

Coenzyme and substrate specificity

The coenzyme specificity of 2,4-DAPDH was examined by measuring enzyme activity using 2,4-DAP as a substrate and either NAD^+ or NADP^+ as the coenzyme. The experiment showed that the enzyme uses both NAD^+ and NADP^+ as a coenzyme (92 and 17 $\mu\text{mol}\cdot\text{min}^{-1}\cdot\text{mg}^{-1}$, respectively). However, the activity of the enzyme with NAD^+ was 5.4 times higher than that with NADP^+ . Therefore, the enzyme prefers to use NAD^+ as a coenzyme.

The substrate specificity of the enzyme during NAD^+ -dependent oxidative deamination was examined using 0.5 mM 2,4-DAP or 2,5-DAH. 2,5-DAH is produced by lysine 5,6-aminomutase,

which catalyzes the 5,6-rearrangement of the terminal amino group of D-lysine in the lysine degradation pathway (Fig. 1). 2,4-DAPDH from *F. nodosum* acted not only on 2,4-DAP (92 $\mu\text{mol}\cdot\text{min}^{-1}\cdot\text{mg}^{-1}$) but also on 2,5-DAH (1 $\mu\text{mol}\cdot\text{min}^{-1}\cdot\text{mg}^{-1}$). The activity of the enzyme using 2,4-DAP as a substrate was approximately 90 times higher than that using 2,5-DAH.

Kinetic parameters of 2,4-DAPDH

Kinetic analysis of the enzyme was performed using 0.005–1 mM NAD^+ or 0.1–8 mM NADP^+ as a coenzyme. The kinetic parameters determined are shown in Table 2. The K_m value for NAD^+ was about 40 times lower than that for NADP^+ , whereas the V_{\max} and k_{cat} values for NAD^+ and NADP^+ were similar.

The activities of the enzyme were measured at various concentrations of 2,4-DAP and 2,5-DAH. The enzyme displayed non-Michaelis-Menten kinetics with 2,4-DAP as the substrate. Although the enzymatic activity increased as the 2,4-DAP concentration increased over the range of 0–0.8 mM, it decreased at 2,4-DAP concentrations over 0.8 mM (Fig. 4). This behavior is consistent with complete uncompetitive substrate inhibition, and the experimental data are fitted well by the equation describing this type of inhibition (Equation 1 in the Materials and Methods). An apparent K_i value and K_m value were calculated as 0.9 mM and 0.2 mM, respectively (Table 2). In contrast, the enzyme displayed typical Michaelis-Menten kinetics when 2,5-DAH (0–10 mM) was used as the substrate (Fig. 5). The kinetic parameters for these substrates are summarized in Table 2.

Regulation of 2,4-DAPDH

We examined whether the activity of 2,4-DAPDH is affected by D-ornithine and D-alanine, which occur as metabolites in the oxidative ornithine degradation pathway (Fig. 1). Enzyme activity was measured in a solution of 50 mM HEPES pH 8.5, 1 mM NAD^+ , and 0.3 mM 2,4-DAP in the presence or absence of these amino acids. Enzymatic activity decreased to 14% and 71% of the

297 positive control in the presence of 5 mM D-ornithine and D-alanine, respectively. We also examined
298 whether D-lysine affects enzyme activity under these same conditions. The activity decreased to 68%
299 of the positive control following the addition of 5 mM D-lysine. Therefore, the activity of 2,4-DAPDH
300 is suppressed in the presence of D-ornithine, D-alanine, and D-lysine. D-Ornithine is the most effective
301 inhibitor. To further characterize the inhibition by D-ornithine, enzyme activity toward 2,4-DAPDH
302 was measured in the presence of varying concentrations of D-ornithine. In double-reciprocal plots of
303 enzyme activity versus 2,4-DAP concentration, a set of parallel linear lines were obtained (Fig. 6),
304 indicating that D-ornithine acts as an uncompetitive inhibitor of 2,4-DAPDH. The apparent K_i value
305 was 0.1 mM.

306

307

Discussion

In this paper, the gene cloning, expression, and characterization of a thermostable 2,4-DAPDH from the thermophilic bacterium *F. nodosum* Rt17-B1 are described. The gene from this bacterium, *Fnod_1646*, was predicted to encode a 2,4-DAPDH. The protein, which was purified from recombinant *E. coli* cells, showed a molecular mass of 38 kDa on SDS-PAGE and catalyzed the oxidative deamination of 2,4-DAP in an NAD(P)⁺-dependent manner. The optimum pH for 2,4-DAP oxidation was in the alkaline range. A variety of metals, such as Cu²⁺, Ni²⁺, and Zn²⁺, inhibited its catalytic activity. This 2,4-DAPDH is noteworthy because it has a high optimal temperature and is thermostable. The optimal temperature for this enzyme in 2,4-DAP oxidation was 85°C. Therefore, the enzyme is an NAD(P)⁺-dependent thermophilic alkaline amino acid dehydrogenase.

We found that besides 2,4-DAP, 2,5-DAH can also serve as the substrate for 2,4-DAPDH (Table 2). 2,5-DAH may be produced from D-lysine by lysine-5,6-aminomutase (14), raising the possibility that 2,4-DAPDH also participates in lysine degradation (Fig. 1). However, the k_{cat}/K_m value of 2,4-DAPDH for 2,5-DAH is much lower than that for 2,4-DAP, implying that 2,5-DAH is not a physiological substrate of 2,4-DAPDH. The validity of this interpretation should be verified in future *in vivo* studies.

In this study, we found notable regulatory properties of 2,4-DAPDH, including uncompetitive substrate inhibition by 2,4-DAP and uncompetitive inhibition by D-ornithine. These results suggest that the oxidative degradation of ornithine is regulated by upstream metabolites; at high concentrations of D-ornithine and 2,4-DAP, this degradation pathway is suppressed. It is known that substrate inhibition of enzymes, such as tyrosine hydroxylase, plays a role in stabilizing the reaction rate against large fluctuations in substrate concentration (15). Therefore, upstream regulation of the oxidative ornithine degradation pathway may result in a steady synthesis of downstream metabolites, such as the D-alanine that is required for the synthesis of peptidoglycan (16, 17), under conditions at which the concentrations of the upstream metabolites fluctuate.

The regulation of 2,4-DAPDH may also affect the metabolic fate of ornithine, which may be metabolized via four different pathways, as analysis of the *F. nodosum* genome and previous reports suggested the occurrence of four ornithine metabolic pathways in this bacterium. The first is the oxidative degradation pathway that was the focus of this study. The second is a spermidine and spermine biosynthesis pathway, which starts with the conversion of L-ornithine into putrescine by ornithine decarboxylase. Polyamines, such as spermidine and spermine, are polycationic compounds that are implicated in a wide variety of biological reactions, including the synthesis of nucleobases and proteins (20). The third is the urea cycle in which ornithine is metabolized by ornithine carbamoyltransferase (19). The fourth is the reductive degradation pathway in which ornithine is reduced to 5-aminovalerate through the formation of proline (5). This reductive pathway has been found in anaerobic bacteria such as *C. sticklandii* (18). Inhibition of 2,4-DAPDH by the upstream metabolites in the oxidative ornithine degradation pathway may direct the metabolic flux of L-ornithine to other pathways. This should be examined in future studies by *in vivo* experiments.

Amino acid dehydrogenases are useful for the synthesis of chiral amino acids from the corresponding keto acids. Because most amino acid dehydrogenases characterized thus far catalyze the interconversion between α -amino acids and α -keto acids, this method has only been used for the production of chiral α -amino acids. Based on its activity toward 2,4-DAP and 2,5-DAH, 2,4-DAPDH should catalyze the reductive amination of the carbonyl group at the γ -position and the δ -position, which differs from the activity of most previously characterized amino acid dehydrogenases. In a preliminary experiment, we tested the reductive amination of 2,4-DAPDH using the oxidative deamination product of 2,4-DAP. After 2,4-DAP was converted to AKP, the reaction was stopped by heat treatment, and AKP was used as the substrate for reductive amination reaction. 2,4-DAPDH catalyzed the AKP-dependent oxidation of NADH, implying that the enzyme catalyzed the reductive amination of AKP (data not shown). Therefore, 2,4-DAPDH is expected to expand the range of chiral amine compounds (other than α -amino acids) produced by amino acid dehydrogenases. When

358 considering such applications, the thermostability of the enzyme is beneficial. Possible applications in
359 the synthesis of chiral amine compounds for the thermostable 2,4-DAPDH identified in this study are
360 currently under investigation.

361

362 Acknowledgments

363 This work was supported in part by the Collaborative Research Program of Institute for Chemical
364 Research, Kyoto University (grant # 2013-59).

365

366

367 References

368

- 369 1. **Somack, R. and Costilow, R. N.:** 2,4-Diaminopentanoic acid C₄ dehydrogenase.
370 Purification and properties of the protein, J. Biol. Chem., **248**, 385-388 (1973).
- 371 2. **Dyer, J. K. and Costilow, R. N.:** 2,4-Diaminovaleric acid: an intermediate in the anaerobic
372 oxidation of ornithine by *Clostridium sticklandii*, J. Bacteriol., **101**, 77-83 (1970).
- 373 3. **Tsuda, Y. and Friedmann, H. C.:** Ornithine metabolism by *Clostridium sticklandii*.
374 Oxidation of ornithine to 2-amino-4-ketopentanoic acid via 2,4-diaminopentanoic acid; participation
375 of B₁₂ coenzyme, pyridoxal phosphate, and pyridine nucleotide, J. Biol. Chem., **245**, 5914-5926
376 (1970).
- 377 4. **Barker, H. A.:** Amino acid degradation by anaerobic bacteria, Annu. Rev. Biochem., **50**,
378 23-40 (1981).
- 379 5. **Fonknechten, N., Perret, A., Perchat, N., Tricot, S., Lechaplais, C., Vallenet, D., Vergne,**
380 **C., Zaparucha, A., Le Paslier, D., Weissenbach, J., and Salanoubat, M.:** A conserved gene cluster
381 rules anaerobic oxidative degradation of L-ornithine, J. Bacteriol., **191**, 3162-3167 (2009).
- 382 6. **Chen, H. P., Lin, C. F., Lee, Y. J., Tsay, S. S., and Wu, S. H.:** Purification and properties of
383 ornithine racemase from *Clostridium sticklandii*, J. Bacteriol., **182**, 2052-2054 (2000).
- 384 7. **Somack, R. and Costilow, R. N.:** Purification and properties of a pyridoxal phosphate and
385 coenzyme B₁₂ dependent D- α -ornithine 5,4-aminomutase, Biochemistry, **12**, 2597-2604 (1973).
- 386 8. **Jeng, I. M., Somack, R., and Barker, H. A.:** Ornithine degradation in *Clostridium*
387 *sticklandii*; pyridoxal phosphate and coenzyme A dependent thiolytic cleavage of
388 2-amino-4-ketopentanoate to alanine and acetyl coenzyme A, Biochemistry, **13**, 2898-2903 (1974).
- 389 9. **Torres-Gavilán, A., Escalante, J., Regla, I., López-Munguía, A., and Castillo, E.:**
390 'Easy-on, easy-off' resolution of chiral 1-phenylethylamine catalyzed by *Candida antarctica* lipase B,
391 Tetrahedron: Asymmetry, **18**, 2621-2624 (2007).

- 392 10. **Pilissão, C., Carvalho, P. O., and Nascimento, M. G.:** Enantioselective acylation of
393 (*RS*)-phenylethylamine catalysed by lipases, *Process Biochem.*, **44**, 1352-1357 (2009).
- 394 11. **Koszelewski, D., Tauber, K., Faber, K., and Kroutil, W.:** ω -Transaminases for the
395 synthesis of non-racemic α -chiral primary amines, *Trends Biotechnol.*, **28**, 324-332 (2010).
- 396 12. **Tufvesson, P., Lima-Ramos, J., Jensen, J. S., Al-Haque, N., Neto, W., and Woodley, J. M.:**
397 Process considerations for the asymmetric synthesis of chiral amines using transaminases,
398 *Biotechnol. Bioeng.*, **108**, 1479-1493 (2011).
- 399 13. **Patel, B. K. C., Morgan, H. W., and Daniel, R. M.:** *Fervidobacterium nodosum* gen. nov.
400 and spec. nov., a new chemoorganotrophic, caldoactive, anaerobic bacterium, *Arch. Microbiol.*, **141**,
401 63-69 (1985).
- 402 14. **Stadtman, T. C.:** Lysine metabolism by Clostridia, *Advance in Enzymology and Related*
403 *Areas of Molecular Biology*, **38**, 413-448 (1973).
- 404 15. **Reed, M. C., Lieb, A., and Nijhout, H. F.:** The biological significance of substrate
405 inhibition: a mechanism with diverse functions, *Bioessays*, **32**, 422-429 (2010).
- 406 16. **van Heijenoort, J.:** Formation of the glycan chains in the synthesis of bacterial
407 peptidoglycan, *Glycobiology*, **11**, 25R-36R (2001).
- 408 17. **van Heijenoort, J.:** Recent advances in the formation of the bacterial peptidoglycan
409 monomer unit, *Nat. Prod. Rep.*, **18**, 503-519 (2001).
- 410 18. **Kenklies, J., Ziehn, R., Fritsche, K., Pich, A., and Andreessen, J. R.:** Proline biosynthesis
411 from L-ornithine in *Clostridium sticklandii*: purification of Δ^1 -pyrroline-5-carboxylate reductase, and
412 sequence and expression of the encoding gene, *proC*, *Microbiology*, **145**, 819-826 (1999).
- 413 19. **Legrain, C., Stalon, V., Noullez, J. P., Mercenier, A., Simon, J. P., Broman, K., and**
414 **Wiame, J. M.:** Structure and function of ornithine carbamoyltransferases, *Eur. J. Biochem.*, **80**,
415 401-409 (1977).
- 416 20. **Tabor, C. W. and Tabor, H.:** Polyamines in microorganisms, *Microbiol. Rev.*, **49**, 81-99

417 (1985).

418

419

Figure Legends

Figure 1. The ornithine oxidative degradation pathway and putative lysine degradation pathway. Ornithine racemase, D-ornithine 4,5-aminomutase, 2,4-diaminopentanoate dehydrogenase, 2-amino-4-ketopentanoate thiolase, lysine racemase, and D-lysine 5,6-aminomutase catalyze reactions 1, 2, 3, 4, 5, and 6 respectively. Reaction 7 is non-enzymatic intramolecular cyclization.

Figure 2. Effect of pH on the activity of the 2,4-DAPDH from the thermophilic anaerobic bacterium, *F. nodosum* Rt17-B1. Enzyme assays were performed using 0.5 mM 2,4-DAP as the substrate in 50 mM acetate (filled circles), 50 mM KPB (open squares), HEPES-NaOH (filled triangles), and CHES-NaOH (filled diamonds) as described in the Materials and Methods. Error bars represent the standard deviation of three independent experiments.

Figure 3. Effect of temperature on the activity of 2,4-DAPDH. Enzyme assays were performed using 0.5 mM 2,4-DAP as the substrate in 50 mM HEPES-NaOH (pH 8.5) at different temperatures as described in the Materials and Methods. Error bars represent the standard deviation of three independent experiments.

Figure 4. Substrate inhibition of 2,4-DAPDH by 2,4-DAP. 2,4-DAPDH activity is plotted as a function of 2,4-DAP concentration. The solid line is a fit to the data (filled circles) according to Equation 1 in the Materials and Methods.

Figure 5. Activity of 2,4-DAPDH toward 2,5-DAH. 2,4-DAPDH activity was plotted as a function of 2,5-DAH concentration. The solid line is a fit to the data (filled diamonds) according to the Michaelis-Menten equation.

445 Figure 6. Inhibition of 2,4-DAPDH by D-ornithine. Double-reciprocal plots were generated at the
446 following D-ornithine concentrations: 0 mM (filled diamonds), 0.5 mM (open circles), 1.5 mM (filled
447 triangles), and 2.0 mM (open squares).

448

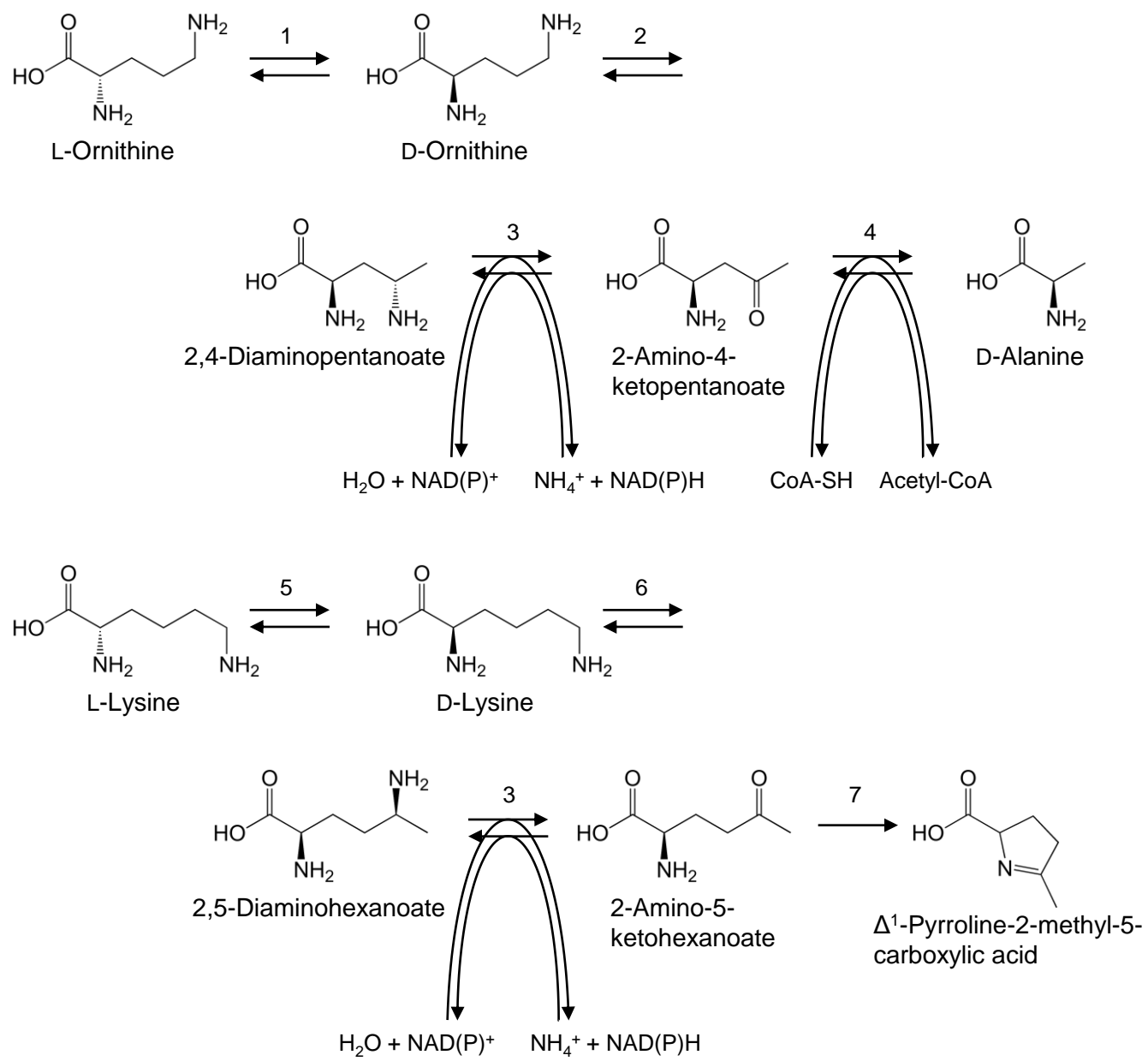


Figure 1

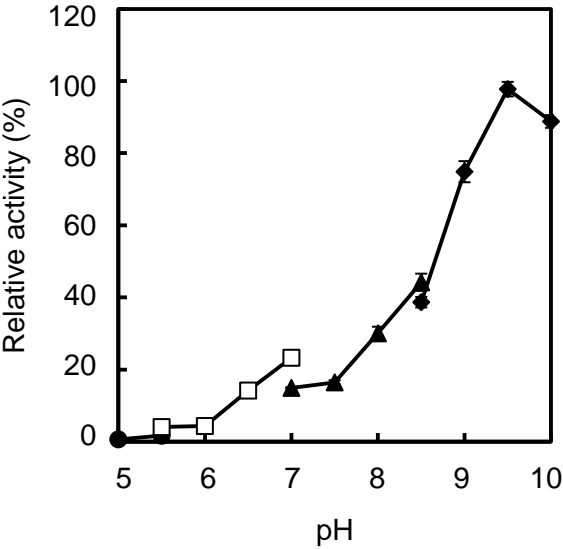


Figure 2

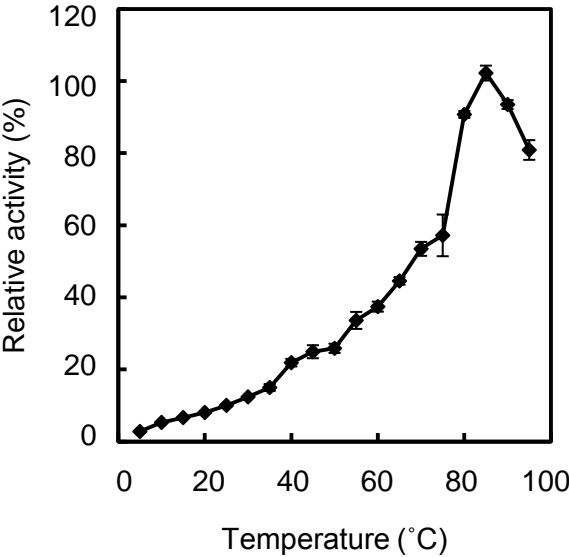


Figure 3

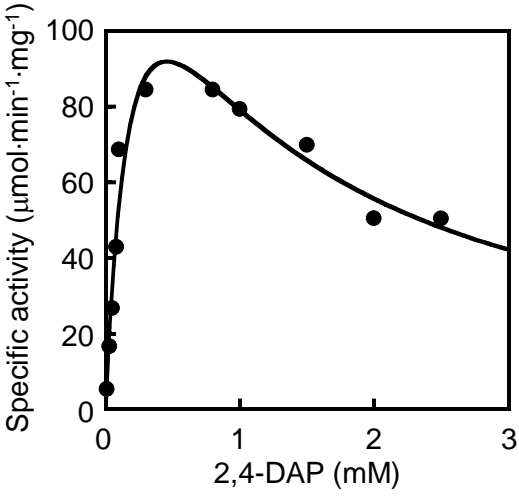


Figure 4

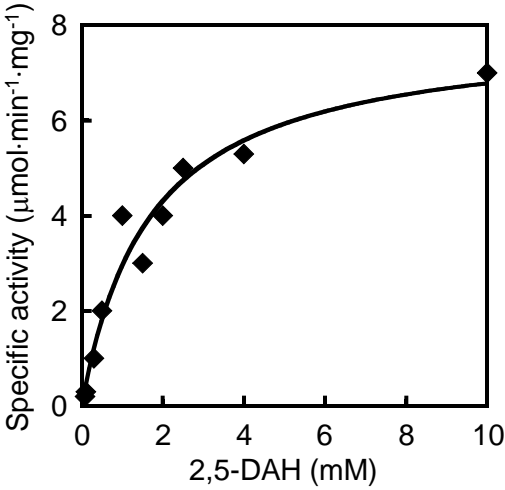


Figure 5

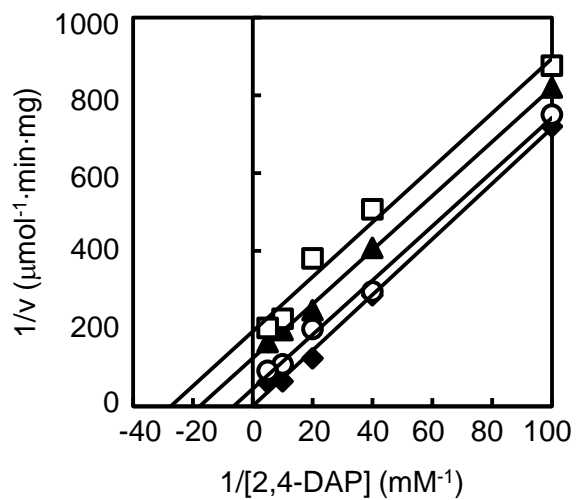


Figure 6

1 Table 1. Effects of various reagents on the activity of 2,4-DAPDH

	Relative activity (%) ^a
None	100 ± 0
EDTA	98 ± 6
MgSO ₄	65 ± 11
CaCl ₂	85 ± 7
FeCl ₂	84 ± 4
MnCl ₂	104 ± 0
CoSO ₄	34 ± 4
NiSO ₄	2 ± 1
CuSO ₄	0 ± 0
ZnSO ₄	2 ± 2
KCl	97 ± 4
KBr	97 ± 5
KNO ₃	93 ± 2
CH ₃ COOK	96 ± 4
K ₂ SO ₄	96 ± 5

2 ^a The values are shown as the mean ± standard deviation of three independent experiments.

1 Table 2. Kinetic parameters of 2,4-DAPDH

	K_m (mM)	K_i (mM)	V_{\max} ($\mu\text{mol}\cdot\text{min}^{-1}\cdot\text{mg}^{-1}$)	k_{cat} (s^{-1})	k_{cat}/K_m ($\text{mM}^{-1}\cdot\text{s}^{-1}$)
NAD ⁺	0.05	-	97	65	1,300
NADP ⁺	2	-	86	57	29
2,4-DAP	0.2	0.9	180	65	330
2,5-DAH	2	-	0.9	0.0006	0.0003

2